Stem Cell Research 15 (2015) 643–654

Contents lists available at ScienceDirect

Stem Cell Research

journal homepage: www.elsevier.com/locate/scr

Short-term uvb-irradiation leads to putative limbal stem cell damage and niche cell-mediated upregulation of macrophage recruiting cytokines☆

Maria Notara *, Refaian N., Braun G., Steven P., Bock F., Cursiefen C.

Dept. of Ophthalmology, University of Cologne.

ARTICLE INFO

Article history:
Received 8 July 2015
Accepted 16 October 2015
Available online 19 October 2015

Keywords:
Limbal stem cells
Limbal niche
Ultraviolet B irradiation
Corneal angiogenesis
Angiogenesis proteins
Pro-inflammatory cytokines

ABSTRACT

Ultraviolet light B (UVB)-irradiation is linked to various ocular pathologies such as limbal stem cell defects in pterygium. Despite the large circumstantial evidence linking UVB irradiation and limbal epithelial stem cell damage, the precise molecular responses of limbal stem cells to UVB irradiation are unclear. Here the effect of UVB irradiation on the putative stem cell phenotype, limbal niche cells and the subsequent effects on corneal (lymph)angiogenic privilege were investigated. Primary human limbal epithelial stem cells and fibroblasts were irradiated with 0.02 J/cm^2 of UVB, a low dose corresponding to 3 min of solar irradiation. UVB irradiation caused significant reduction of limbal epithelial and limbal fibroblast proliferation for 24 h, but apoptosis of limbal epithelial stem cells only. Moreover, UVB induced stem-like character loss of limbal epithelial cells, as their colony forming efficiency and putative stem cell marker expression significantly decreased. Interestingly, limbal epithelial cells co-cultured with UVB-irradiated limbal fibroblasts also exhibited loss of stem cell character and decrease of colony forming efficiency. Conditioned media from limbal epithelial cells inhibited lymphatic endothelial cell proliferation and tube network complexity; however this effect diminished following UVB irradiation. In contrast, pro-inflammatory and macrophage-recruiting cytokines such as TNFα, IFNγ and MCP1 were significantly upregulated following cell irradiation of limbal fibroblasts. These data demonstrate the key role of the limbal stem cell niche in response to UVB and subsequent (lymph)angiogenic and inflammatory events. These data suggest that the known pro(lymph)angiogenic effect of UVB irradiation in pterygium is not linked to a direct up-regulation of pro-angiogenic cytokines, but rather to indirect macrophage-recruiting cytokines being upregulated after UVB irradiation.

1. Introduction

UV radiation (UVR) is damaging for the eye resulting to a reduction or even loss of vision. The cornea is particularly susceptible to UVR due to its natural transparency and its shape which is contributing to a peripheral light focusing effect, affecting the nasal limbus where UV irradiation is 20-fold strongest (Coroneo et al., 1991; Maloof et al., 1994). This is the most frequent site for the onset of pterygium, a non-cancerous growth of the cornea, usually bilateral, which is occupying the corneal equator. The pterygium disrupts the limbal barrier which separates the cornea from the conjunctiva and centripetally invades the cornea surface. It is characterised by squamous hyperplasia and goblet cell hyperplasia. In advanced cases, the visual axis may be covered by vascularised opaque tissue thus leading to discomfort, deterioration of vision or even blindness (Bradley et al., 2010).

As such dramatic phenotype change occurs in the limbus and its adjacent tissues, alterations in the limbal stem cell niche and its resident limbal epithelial stem cells (LESC) must also occur. LESCs play a key role in the maintenance of cornea transparency and homeostasis by replenishing its outermost layer, the epithelium (Notara et al., 2010a). If these stem cells become depleted by injury or disease, the neighbouring conjunctival epithelium infringes onto the corneal surface causing vascularisation, persistent epithelial breakdown, severe pain and blindness (Notara & Daniels, 2008). Although a LESC-specific marker remains elusive, the expression of certain proteins, including P63α, ABCG2, and cytokeratin 15 and more recently ABCB5 (Ksander et al., 2014) have been recognised as putative stem cell markers for these cells (Notara & Daniels, 2008). High levels of putative stem cell marker expression combined with high colony forming efficiency (CFE) (Barrandon & Green, 1987) are indicative of the stem cell phenotype.

There is strong evidence that pterygium pathogenesis is linked to UVR-induced damage of limbal epithelial stem cells (Chui et al., 2011;

Abbreviations: UVB, Ultraviolet irradiation B; HLE, Human Limbal Epithelial cells; HLF, Human Limbal fibroblasts; BHLE, UVB irradiated Human Limbal Epithelial cells; BHLF, UVB irradiated Human Limbal Epithelial cells; LEC, Lymmphatic vessel Endothelial Cells; BEC, Bloor vessel Endothelial Cells; CFE, Colony Forming Efficiency; CM, Conditioned Medium.

☆ Support: EU COST BM1302 (MN, FB, CC); DFG FOR 2240 (FB, PS, CC); Brunner Foundation Cologne (MN).

* Corresponding author at: Dept. of Ophthalmology, University of Cologne, Kerpener Straße 62, 50937, Cologne, Germany.
E-mail address: maria.notara@uk-koeln.de (M. Notara).

http://dx.doi.org/10.1016/j.scr.2015.10.008

Di Girolamo et al., 2003) and matrix metalloproteinase activation (MMPs) (Dushku & Reid, 1994; Dushku et al., 2001). However, the direct involvement of LESC in the onset and development of the condition or the particular effect of chronic UVR to the phenotype of these stem cells is not fully understood. It is logical to suggest that since stem cells are long cycling and live throughout most of the lifetime of an individual, they can accumulate UV related damage which can lead to benign or even malignant growths. P53 activation has been observed in pterygium and recurrent pterygium specimens, thus suggesting direct DNA damage and activation of the DNA repair mechanism (Cimpean et al., 2013). At the same time, UV damage on LESC niche accessory cells such as limbal fibroblasts may adversely affect the stem cell phenotype and functionality, but again is poorly understood. Overall, the (photo)-ageing of the LESC niche, features both a change in the physical size and appearance of the putative stem cell niche structures located at the palisades of Vogt (which become limited to the light-protected, lid-covered parts of the superior and inferior limbus) as well as a decline in the proliferative efficiency of the LESCs and has been linked to UVR (Notara et al., 2013). In this light, better understanding of the effects of UVB irradiation on the limbal niche and its resident LESCs can lead to improved therapeutic options.

UV-induced changes in the cornea are largely mediated by the up-regulation of pro-inflammatory cytokines such as interleukin (IL)1 (Corsini et al., 1997), IL6 (Di Girolamo et al., 2002), IL8 (Di Girolamo et al., 2002) and tumour necrosis factor alpha (TNFα) (Kennedy et al., 1997) which correlate to the increased inflammatory cell infiltrate associated to the condition. Also increased are growth factors including vascular endothelial growth factor (VEGF) (Fukuhara et al., 2013; Lee et al., 2001), platelet derived growth factor (PDGF) (Kria et al., 1996), transforming growth factor beta (TGFβ) and matrix metalloproteinases (MMP) (Dushku et al., 2001; Di Girolamo et al., 2005; Li et al., 2001), especially MMP1. VEGFC, the master regulator of lymphangiogenesis (Cursiefen et al., 2006), and its receptor VEGFR3 are also up-regulated in pterygium specimen (Fukuhara et al., 2013). This increase correlates to the higher density of lymphatic network associated with pterygium recurrence and staging (Ling et al., 2012a; Ling et al., 2012b).

In this current study, we use an *in vitro* approach to explain the effect of UVB in the phenotype and functionality of human limbal epithelial cells and their accessory limbal fibroblasts as well as their paracrine signaling regulating inflammation and (lymph)angiogenesis.

2. Materials and methods:

2.1. Culturing of 3T3 mouse fibroblasts

A 3 T3 mouse fibroblast cell line, a gift from the lab of professor Nischt (department of dermatology, Uniklinik Köln, Cologne, Germany) were cultured in Dulbecco's Modified Eagle Medium (DMEM, life technologies) supplemented with 10% Fetal Bovine Serum (Gibco) and 1% penicillin/streptomycin/amphotericin (life technologies). Culture medium was refreshed three times per week and the cells were sub-cultured upon reaching 60–70% confluence at a ratio of 1:10. The cultures were kept at 37 °C and 5% CO_2 in air. To be used as a feeder layer for the culture of corneal epithelial cells, the 3 T3 cells were treated in culture medium containing 6 μg/ml mitomycin C (Sigma) for 3 h.

2.2. Ethics statement:

Research consented human cadaveric corneoscleral rims and buttons, a surplus of surgery, were used for cell isolation according to the declaration of Helsinki.

2.3. Primary human limbal epithelial cell harvesting and maintenance

Human limbal epithelial (HLE) cells were cultured in medium containing DMEM F12 (1:1) (Life Technologies) with added 10% Fetal Bovine Serum, 1% penicillin/streptomycin/amphotericin (Life Technologies), 5 μg/ml human recombinant insulin (Sigma), 0.1 nM cholera toxin B (Sigma), 0.05 mM hydrocortisone (Sigma) and 10 ng/ml epidermal growth factor (Life Technologies). Culture medium was refreshed three times a week. HLE cells were isolated from research consented corneas supplied by the Lion's Cornea Bank (University of Cologne, Cologne). Whole corneo-scleral buttons or limbal rims were immersed in a 1.2 U/ml dispase II solution (Sigma) for 2 h at 37 °C or overnight at 4 °C. After the enzymatic treatment, the tissue segments were transferred into a 10 cm petri dish. The epithelial cells were gently scraped by using a feathered scalpel and aiming at the limbal border to achieve an enriched LESC/progenitor population. The cells were collected using 5 ml epithelial culture medium and then placed into a T-25 tissue culture flask (Nunc) containing a feeder layer of growth arrested 3 T3 fibroblasts at a cell density of $2.4x10^4$ cells/cm^2. The cultures were kept at 37 °C and 5% CO_2 in air. Epithelial colonies were observed after 3–5 days.

2.4. Isolation and culture of human limbal fibroblasts

After isolating epithelial cells for culture, as described before (Lee et al., 2001; Kria et al., 1996), the scleral and corneal part of the rims were cut off to leave approximately 1 mm on either side of the limbus. Subsequently, the tissue was further dissected in to smaller fragments. These pieces were allowed to adhere, epithelial side down, on to 10 cm petri dishes. The explants were subsequently cultured in DMEM (Invitrogen) plus 10% FBS and 1% penicillin–streptomycin (Invitrogen) until fibroblasts emerged. The cells were sub-cultured after approximately 2–3 weeks. The cells were passaged at a ratio of 1:2 and the medium was changed 3 times per week.

2.5. Serum-free epithelial-fibroblast co-culture model

Limbal fibroblast and limbal epithelial cells were cultured in a 3 to 1 ratio at 4×10^3/cm^2 and 1.2×10^4 cells/cm^2 respectively, as reported before (Notara et al., 2010b). The cultures were grown in the corneal epithelium medium described before omitting the serum. Due to the difference in the time of establishing the primary respective cultures, limbal epithelial and limbal fibroblast cells from different donors were used.

2.6. Maintenance of human lymphatic and blood endothelial cells

Primary human dermal lymphatic endothelial cells (LEC) and blood endothelial cells (BEC) where purchased from PromoCell and were maintained in supplemented ECGM MV2 culture medium according to the manufacturer's instructions. The cells were passaged once reaching 80% confluence by using a Trypsin/EDTA (0.04%/0.03%) solution for 2 min followed by a trypsin neutralizing solution (0.05% Trypsin Inhibitor in 0.1% BSA), both by Promocell. The cells were used until passage 8.

2.7. UVB-irradiation of cells and collection of conditioned medium

Limbal epithelial and limbal fibroblasts were plated in 2 × 10 cm Petri dishes per type, one to be subjected to UVB irradiation (from this point referred to as BHLE and BHLF respectively) and the other one to be used as a control. To avoid the use of feeder cells, HLE cells were expanded as described in the sections above and were separated from their feeder 3 T3 cells using differential trypsinisation. Subsequently, they were plated in a commercially available serum-free corneal epithelial culture media which does not require the use of feeders, CNT-50 (CellnTech), while the HLF cells were placed in their normal culture media (DMEM supplemented with 10%FBS and 1% pen-strep). The cultures were left to reach approximately 90% confluence. Prior to irradiation, the culture media was replaced with PBS. A Vilber Lourmat, Bio-Sun. UV irradiator set at 265 nm was used to irradiate the cultures at 20 mJ/cm^2 (the equivalent of UVB received during 3 min of sun

exposure) as previously reported (Di Girolamo et al., 2002). The PBS was replaced with their respective culture medium and the cultures were left for 24 h to settle. Then, cells were plated in 6 well plates at a seeding density of 10^5 cells per well. One day later, the culture medium was replaced with MV2 basal endothelial medium with added 2% FBS (basal medium BM). The produced conditioned media were collected after 24 h, centrifuged at 1500G to clarify from dead cells and debris, aliquoted and stored at −80 °C for a maximum of 2 months before use.

2.8. FACS analysis

Antibody labeling of single cell suspensions was performed in PBS with added 2% FBS, and 10 mM HEPES for 20 min against appropriately matched-isotype controls. Cell apoptosis was assessed by using a fluorescein isothiocyanate (FITC)-conjugated Annexin 5 system according to the manufacturer's instructions (Biolegend). The stained cells were re-suspended in 600ul PBS, 2% FCS, 10 mM HEPES, and 4 ul 7AAD (to detect dead cells, biolegend) and passed through a 40-um mesh before analysis in a FACS Calibur (Becton Dickinson biosciences). Data processing was performed using FlowJo (Tree Star). These experiments were carried out with cells from 3 different donors.

2.9. Immunocytochemistry of cells

Eight-well permanox chambered slides (labtek, Nunc) were used for immunocytochemistry of cultured cells. The cells were washed three times with PBS, fixed for 10 min at room temperature in 4% (wt/vol) paraformaldehyde and in case of not performing the staining immediately they were treated with 20% (wt/vol) sucrose before storage at −20 °C.The samples were blocked for 1 h in PBS supplemented with 5% goat serum (Sigma) and 0.5% Triton X (Sigma) followed by the primary antibody (cytokeratin (K)15 antibody from Santa Cruz (clone LHK15, catalogue number sc-47,697), rabbit polyclonal integrin beta 1 antibody from Abcam (catalogue number ab183666), mouse monoclonal antibody for cytokeratin (K)3 from Millipore (clone AE5, catalogue number CBL218) and rabbit polyclonal antibody for p63α from new England biolabs (catalogue number 4892S) or blocking reagent only (negative control) overnight at 4 °C. Subsequently, the cells were incubated with their respective secondary antibody (goat anti-rabbit alexa 488, goat anti mouse alexa 647, both from Life Technologies), washed and counterstained with DAPI. All incubations apart from the primary antibody incubation were performed at room temperature, and each step was intermittent with 3 × 5 minute rinses with PBS containing 0.1% tween-20 (Sigma). Negative controls were treated in the same way except omitting the primary antibody step. All stainings were repeated with cells from at least 3 different donors.

2.10. Colony forming efficiency assay

For the colony forming efficiency (CFE) assay (Notara et al., 2013; Notara et al., 2010b), 3 T3 fibroblasts were used as a feeder layer. The cells were treated with mitomycin C as above and plated at a cell density of 4.8 x 10^5 cells in each well of a six well plate and were allowed to attach overnight. HLE were seeded at a cell density of 1000 cells per well of the six well plate. The cultures were fixed with cold methanol for 20 min at −20 °C at day 12. Subsequently, the cells were stained with a solution of 1% rhodamine B (Sigma) and 1% Toluidine Blue (Gurr) for 30 min at 37 °C. Finally, the plates were photographed and Image J software was used to count the number of colonies that measured greater than 2 mm diameter. The percentage of colony forming efficiency was calculated by using the equation:

$$\mathrm{CFE}(\%) = \frac{\text{Number of colonies}>2\text{mm}}{\text{Number of cells seeded}} \times 100$$

The experiments were carried out with cells from three different donors (n = 6).

2.11. Cell metabolic activity

Cell metabolic activity was assessed using the alamar blue assay (Thermo Scientific). Limbal epithelial cells and limbal fibroblasts were cultured in 10 cm petri dishes and were UVB-irradiated as described in the section above. Then, 24 h after the UVB irradiation, the cells were plated in 96 well plates at a cell density of 5x10^3 cells per well in a minimum of 5 replicates. The alamar blue assay was carried out the following day.

For the LEC and BEC cells, these too were plated in 96 well plates at cell density of 5000 cells/well and were left to settle overnight. Then, the endothelial culture medium was replaced with the various CM and the cells were left for another 24 h before carrying out the alamar blue assay.

To perform the assay, the cultures were incubated for 1 h in 150 μl/well alamar blue reagent diluted 10 times in PBS (with n = 5 at minimum). Cell-free wells with added alamar blue reagent were used as blanks. After incubation, the plates were analysed in an Epoch plate reader (Biotech) in absorbance mode at 570 nm and 600 nm and the percentage of reduction of the alamar blue reagent was calculated as suggested in the manufacturer's instructions. These experiments were repeated with cells from at least 6 different donors.

2.12. Scratch wound assay

Scratch wound assays were carried out, as described previously (Ling et al., 2012a). Briefly, LEC or BEC were plated to complete confluence in a 96 well plate, serum-starved for 2 h and scratch-wounded using a 10 μl pipette tip (n = 5). Then, the cells were treated with the various CM (produced as described in a previous section). Here too, as a control, LEC or BEC CM was used respectively (spent medium). The wounds were photographed at 0, 2 and 6 h for BEC and 0, 8 and 16 h for LEC to accommodate for the slower wound closure rate of the latter. The wound surface areas at each time-point were measured using Image J software. The data of each replicate were presented as a percentage of healed wound area compared to the original wound area at 0 h. The experiments were repeated at least 5 times with different CM.

2.13. Tube formation assay

The tube formation assays were performed on Matrigel® (Corning) in μ-Slide angiogenesis assay (Ibidi) according to the manufacturer's instructions. BEC or LEC were seeded at a cell density of 1x10^4/well in complete endothelial cell medium. One hour later the cells fully adhered on the Matrigel® and the full medium was replaced with the supernatants and control media (n = 5). The formed tube networks formed were photographed after 16 h using a Zeiss Primo Vert inverted microscope fitted with an AxioCam ERc5s camera. The number of branches, loops and branching points were quantified using the Lymphatic Vessel Analysis Protocol (LVAP) plugin (Roberts, 2011) in Image J (Yam & Kwok, 2014) software.

2.14. Protein microarray

CM from all groups was collected as described above and subsequently analyzed in a Proteome Profiler Human Angiogenesis Array (R&D biosciences) according to the manufacturer's instructions. The arrays were visualized using a ChemiDoc™XRS + System.

2.15. Elisa

ELISA kits from R&D biosciences were used for protein analysis according to the manufacturer's instructions. Angiogenin, IGBP-3,

TNFα, MCP1 and IFNγ were quantified using the respective human Quantikine® ELISA while VEGFA and VEGFC were analyzed by using the corresponding human DuoSet®. Each sample was analyzed in triplicate. The proteins were quantified in conditioned medium from at least three donors.

2.16. Statistical analysis

Statistical analysis of results was carried out using Prism 6.0 software (GraphPad). One-way Analysis of Variance (ANOVA) with Tuckey's multiple comparisons test was used. Sets of data producing $p < 0.05$ were considered statistically significant. As explained in the sections above the experiments were performed using a minimum of 3 experimental triplicates and repeated at least three times (using cells from three different donors (primary cells) or with 3 different cell passages (LEC and BEC cells). All error bars represent standard deviation values.

3. Results

3.1. UVB irradiation induced apoptosis of limbal epithelial cells, but not limbal fibroblasts

To assess the potential pro-apoptotic effects of UVB on HLE and HLF cells, the levels of annexin V binding 4 h post-irradiation were measured using FACS analysis. The cells were counterstained with 7AAD which is taken up by dead cells. As depicted in Fig. 1, the UVB irradiated HLE cells (BHLE) featured an increase in both apoptotic and dead cells (from 10.4 ± 2.1% to 14.4 ± 2.2% and from 14.8 ± 1.2% to 20.0 ± 2.3% respectively – Fig.1A, upper left and right panels, $p < 0.05$). In contrast, no noticeable change occurred in apoptosis and cell death for BHLF cells (Fig. 1A, lower left and right panels).

3.2. UVB irradiation induced a reduction in metabolic activity of both limbal epithelial cells and limbal fibroblasts

To differentiate between this early pro-apoptotic effect and influences of UVB to the functional properties of the cell populations such as cell proliferation, cells were plated for all assays 24 h post UVB irradiation to ensure that only viable cells are used. 24 h post plating (48 h after irradiation), both BHLE and BHLF cells exhibited a significant drop in their metabolic activity ($p < 0.001$ and $p < 0.05$ respectively). 48 h post-plating this difference was no longer observed (Fig. 1 B and C).

3.3. UVB irradiation induced partial loss of putative stem cell markers and a reduction in the colony forming efficiency of limbal epithelial cells

Together with causing a transient reduction in HLE cell proliferation, UVB affected their putative stem cell phenotype. Specifically, the colony forming efficiency of the irradiated BHLE cells significantly declined compared to the on irradiated HLE (2-fold decrease, $p < 0.05$, Fig. 2A). This also applied for colonies with a diameter larger than 2 mm which are attributed to clones with higher potency ($p < 0.05$, Fig. 2A). At the same time, the BHLE cultures featured areas with a differentiated phenotype consisting of enlarged squamous cells which did not express the putative stem cell markers integrin β1 (Fig. 2 E and F where negative regions are indicated by white arrows), p63a and K15 (Fig. 2 G and H,white arrows highlight the negative regions). In addition, the BHLE cultures exhibited an increase in K3-positive cells or cell clusters which also were also enlarged compared to HLE (Fig. 2 I and J respectively, again white arrows indicate the K3 positive regions).

3.4. UVB irradiation of limbal fibroblasts reduced their ability to inhibit limbal epithelial cell differentiation in a co-culture

Notably, a similar, differentiated phenotype was displayed in parts of HLE cultures which were grown in a co-culture with BHLF cells. HLE cells co-cultured with HLF cells on the other hand, exhibited high nuclear to cytoplasmic ratio and formed tightly packed colonies (Fig. 2B, colony encircled by red dotted line). When co cultured with irradiated HLF, HLE exhibited a flattened, squamous shape correlating to differentiated cell morphology (Fig. 2C, differentiated areas emphasized by yellow arrows).

The cell morphology observations corresponded to colony forming efficiency and marker expression data. Specifically, HLE cultured on irradiated HLF featured a significantly lower CFE compared to control cultures (2-fold decrease, $p < 0.001$), this also applying for colonies

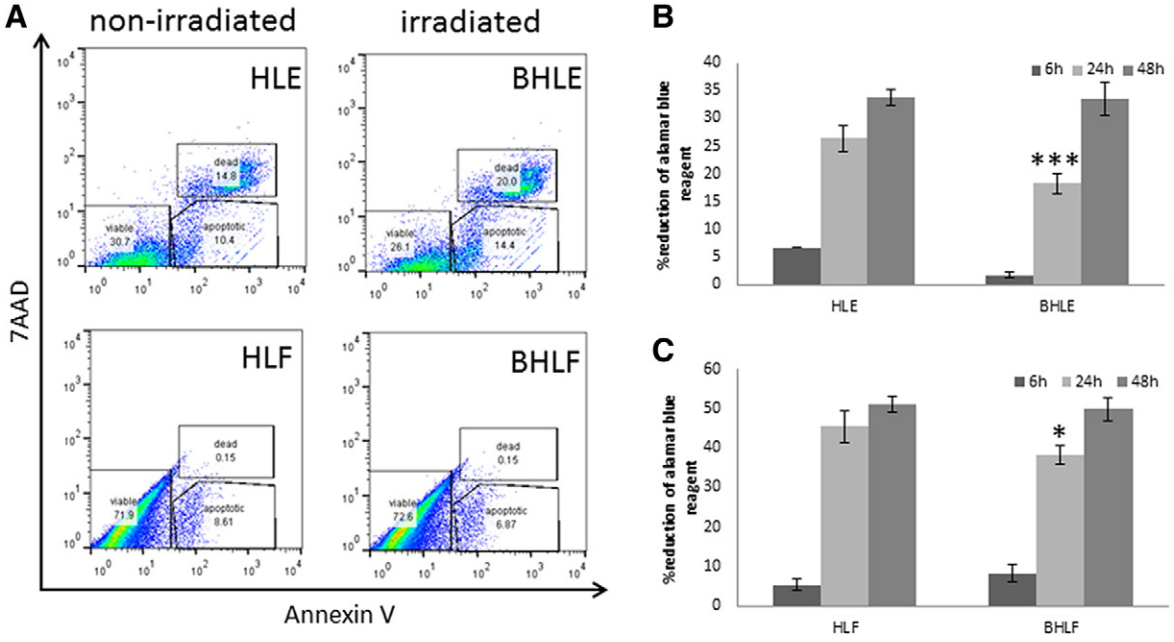

Fig. 1. Impact of UVB on viability, apoptosis and metabolic activity of limbal epithelial cells and fibroblasts. A: FACS analysis of the apoptosis marker Annexin 5 vs the viability marker 7AAD. UVB irradiation reduced limbal epithelial but not limbal fibroblast viability and apoptosis (as measured 4 h after UVB irradiation). B,C: Both UVB treated cell types exhibited a reduction in their metabolic activity at 24 h after plating which was subsequently leveled with their non-irradiated counterparts at 48 h. ($n = 5$, $^{*}p < 0.05$, $^{***}p < 0001$).

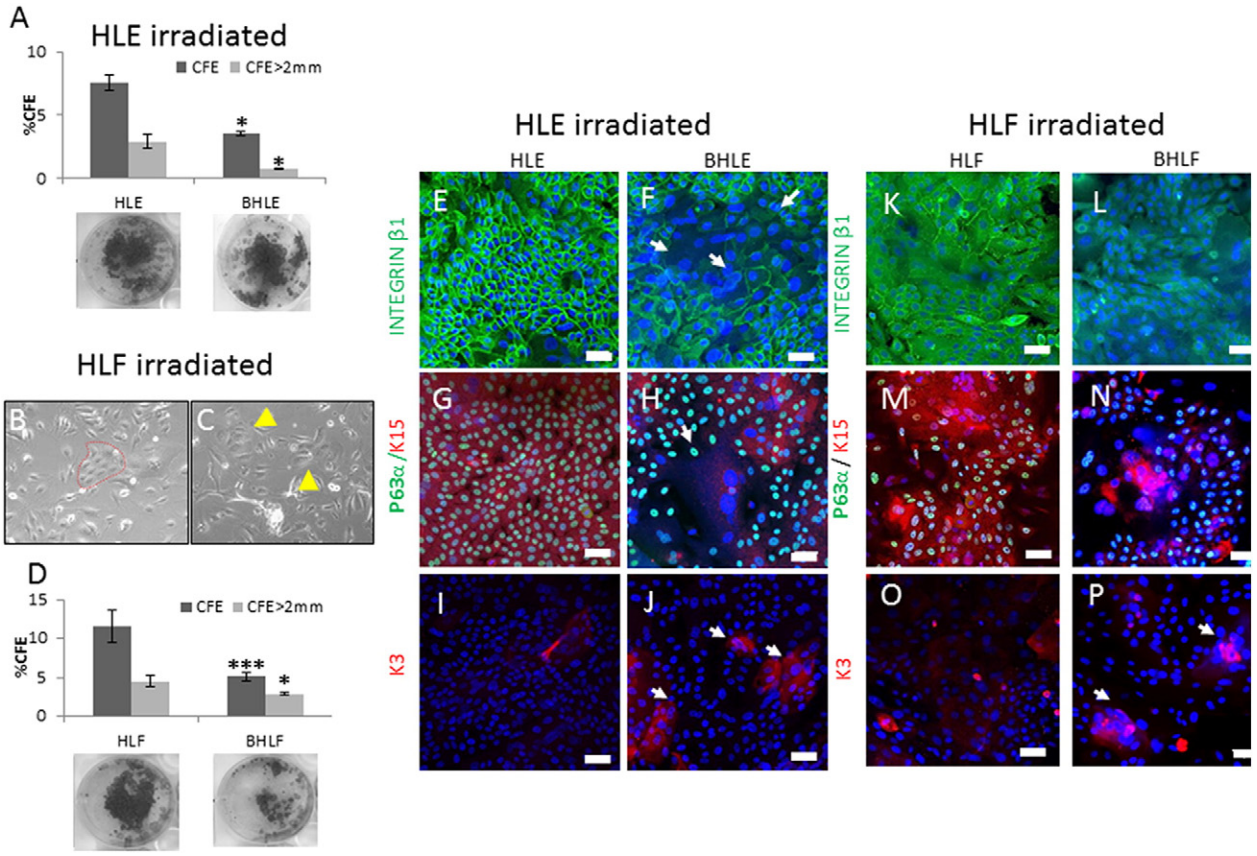

Fig.2. UVB irradiation induced loss of putative stem cell markers causing differentiation of limbal epithelial cells. Colony forming efficiency of irradiated limbal epithelial cells was significantly lower compared to their non irradiated counterparts indicating loss of proliferative potential as a result of ultraviolet B treatment (A). When co-cultured with limbal fibroblasts cells, limbal epithelial cells cells are small, tightly packed and exhibit coblestone morphology (B, 24 h) while when in co-culture with irradiated limbal fibroblasts they display a differentiated phenotype (C, 24 h) and a decreased colony forming efficiency (D). Immunocytochemistry of putative stem cell marker expression including the basal marker integrin β1 (E, F, K and L, alexa488), p63α and K15 (G, H, M and N, alexa488 and alexa647 respectively) and of the mature corneal epithelial marker K3 (I, J and O, P, alexa 647). In irradiated limbal epithelial cells or in limbal epithelial cells co-cultured with irradiated limbal fibroblasts, the markers integrin β1 (F, L) as well as p63α and K15 (H, N) were partially lost (areas indicated by white arrows) while areas expressing the differentiation marker K3 increased (J, P, white arrows highlighted K3-positive regions). For colony fomring efficiency assay: n = 6, $^{*}p < 0.05$, $^{***}p < 0001$. Scale bars correspond to 50 μm.

with a diameter larger than 2 mm ($p < 0.05$, Fig. 2D). Here too, more areas of the cultures were observed where cells were enlarged and putative stem cell marker expression including integrin β1, p63α and K15 was absent (Fig. 2K-N), while the presence of K3 positive cells increased (Fig. 2O-P). It is also noted that the localization of integrin β1 in the serum-free co cultures (Fig. 2 K and L) is more cytoplasmic in contrast to that of serum-containing cultures, were the protein is more restricted to the cellular cortex (Fig. 2 E and F).

3.5. UVB affected the paracrine action of limbal epithelial cells and limbal fibroblasts on lymphatic and blood endothelial cells

To investigate the effect of soluble mediators produced by HLE, BHLE, HLF and BHLF their conditioned media was used to treat LEC and BEC. Their response by means of metabolic activity, wound healing and tube formation ability were evaluated.

In terms of metabolic activity, it was shown that CM from HLF stimulated LEC more compared to CM from HLE and the LEC own CM (used as 'spent' control) ($p < 0.05$ and $p < 0.01$ respectively). CM from BHLF cells on the other hand induced significantly lower levels of LEC metabolic activity compare to CM from HLF ($p < 0.01$) and similar to LEC CM. A reducing trend, however statistically non-significant, was also observed for the CM from BHLE compared to the one from HLE (Fig. 3A).

The metabolic activity observations correlated to the results of the wound healing assay. In fact, the stimulating effect of CM from HLF compared to the one from HLE was consistent at both the 8 h and 16 h timepoints ($p < 0.05$ in both cases). At 16 h, the wound closure of LEC cultured in CM from HLF was significantly higher compared to the CM from BHLF, HLE and LEC ($p < 0.05$, and $p < 0.01$ respectively, Fig. 3B).

A tube formation assay, illustrated in bright-field photos, was carried out to reproduce the ability of LEC cells to form vessels *in vitro* while cultured in CM from HLE, BLE, HLF and BLF (Fig. 3C-F). From these microphotographs it became evident that CM from HLF stimulated the formation of a more complex network compared to other CM (Fig. 3E). Specifically, CM from HLF induced the formation of higher branch number, loop number and branching points compared to CM from both HLE and BHLF ($p < 0.01$ and $p < 0.001$, $p < 0.5$ and $p < 0.01$, $p < 0.5$ and $p < 0.01$ respectively, Fig. 3G-I).

In contrast to LEC, BEC did not display significantly different levels of proliferation or wound closure in response to the different CM (Fig. 4 A and B). Quantification of the assay microphotographs revealed that CM from HLF stimulated a higher number of branches and branching points compared to CM from HLE and BHLF ($p < 0.01$ and $p < 0.05$ Fig. 4 G and I). No significant differences were observed in the number of loops (Fig. 4H).

3.6. Ultraviolet B irradiation of limbal epithelial cells and limbal fibroblasts impacts on soluble mediators regulating inflammation and lymph/hem-angiogenesis

In order to understand the potential effects of the various CM on BEC and LEC functionality, lymphangiogenic and inflammatory signals were investigated by using a proteomic approach (a protein array) and ELISA analyses.

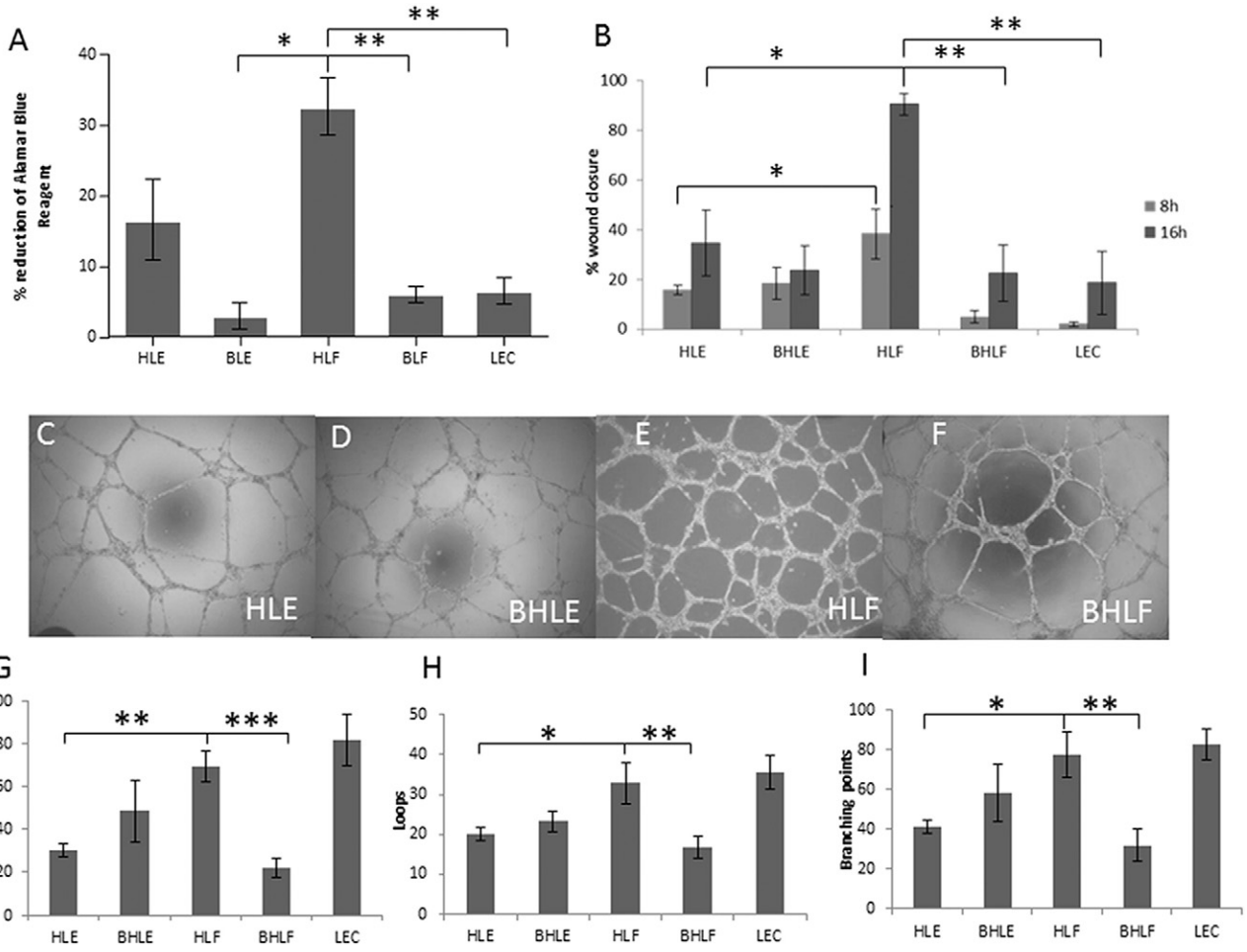

Fig. 3. The promoting paracrine effect of limbal fibroblasts on lymphatic endothelial cells is reversed by UVB. Conditioned media from limbal fibroblasts induced an increase in metabolic activity (A) and wound healing (B, 24 h, 48 h) of lymphatic endothelial cells while this stimulatory effect diminished with ultraviolet B irradiation. A tube formation assay (C-F depict brightfield microphotographs of lymphatic endothelial cells cultured in CM from, irradiated limbal epithelial cells, limbal fibroblasts and irradiated limbal fibroblasts respecively) was used to compare the effect of soluble mediators produced by each group to the complexity of the formed vessel networks. Conditioned media from limbal fibroblasts induced a significantly higher number of branches (G), loops (H) and branching points (I) compared to the ones of limbal epithelial cells and limbal fibroblasts. (for each assay, n = 5, $^{*}p < 0.05$, $^{**}p < 0{,}01$ and $^{***}p < 0001$).

The results from a human angiogenesis protein array are shown in Fig. 5A with a semi-quantitative densitometry analysis on the respective blots of CM from HLE, BHLE, HLF and BHLF. The data are further organised in heat-maps illustrating up-regulations and down-regulations of protein expression levels as well as the corresponding relative intensity fold changes (Fig. 5B). Major relative intensity fold changes (>2-fold) are noted with bold letters. A comparison of CM of HLE with HLF cells demonstrated a major down-regulation for endothelin-1 and amphiregulin (37.9 fold and 4 fold respectively). Smaller changes were observed for IGFB-1, TSP1, TIMP1, CXCL16 and IL8 (all displaying a lower than 2-fold down-regulation). On the other hand, MCP1 was highly upregulated in HLF cells (36-fold) while only small increases were observed for IGFBP-2, uPA and Serpine 1 (1.5, 1.4 and 1.1-fold respectively, Fig. 5B).

The second heat-map features protein level changes in CM of HLE cells and BHLE cells (Fig. 5C). Endothelin1 and amphiregulin levels in BHLE CM were reduced by 37.9 and 4.0-fold while IGFBP-1, TSP1, TIMP1CXCL16 and IL8 were to a lesser extent down-regulated (all by less than 1.6-fold).MCP1 on the other hand was strongly increased by 36-fold,as IGFB-2, uPA and Serpine 1 only increased by less than 1.5-fold (Fig. 5C).

The third heat-map illustrates protein concentration differences between CM from HLF and BHLF (Fig. 5D). Here, a substantial decrease in HLF-secreted amphiregulin, uPA and CXCL16 was noted (20.77, 14.57, 8.28-foldcorrespondingly). Serpine 1, TIMP1 and TSP1 were rather unchanged (each reduced by 1.26, 1.23, and 1.20-fold). MCP-1 was on the other one increased by 2.16-fold while smaller increases were observed for IL8, IGFBP-1, IGFBP-2 and endothelin1 (1.54, 1.47, 1.4 and 1.18-fold respectively).

As a complementary to the protein array, ELISA analyses of more key players of angiogenesis were carried out (Fig. 6 A-D). The proteins angiogenin and IGFBP-3 were selected for further investigation as it was possible to visually observe differences in the protein array blots however not possible to assess them reliably with densitometry due to the increased exposure times required resulting to background. Also, VEGFA, VEGFC and VEGFD which play a fundamental in hem- and lymphangiogenesis were not represented in the array. In all groups, the levels of VEGFD were under the detection range of the assay and therefore these data are not presented.

Angiogenin ELISA data, as depicted in Fig. 6A, illustrated a significant difference between HLE and HLF (2.9-fold, $p < 0.0001$) while BHLF produced significantly less protein than BHLF (1.43-fold $p < 0.01$). In the case of IGFBP-3, shown in Fig. 5F), BHLE featured to have a small (1.4-fold) but significant ($p < 0.0001$) down-regulation compared to HLE. A reduction in BHLF was also noted ($p < 0.05$). A 2-fold increase was shown in IGFBP-3 levels of HLF compared to HLE (Fig. 6 B, $p < 0.0001$). In the case of VEGFA (Fig.6C), BHLE had a (1.6-fold) down-regulation compared to HLE ($p < 0.0001$). A reduction in BHLF compared to BHLF was also noted ($p < 0.0001$). A 2.5-fold increase was shown in VEGFA levels of HLF compared to HLE ($p < 0.0001$).

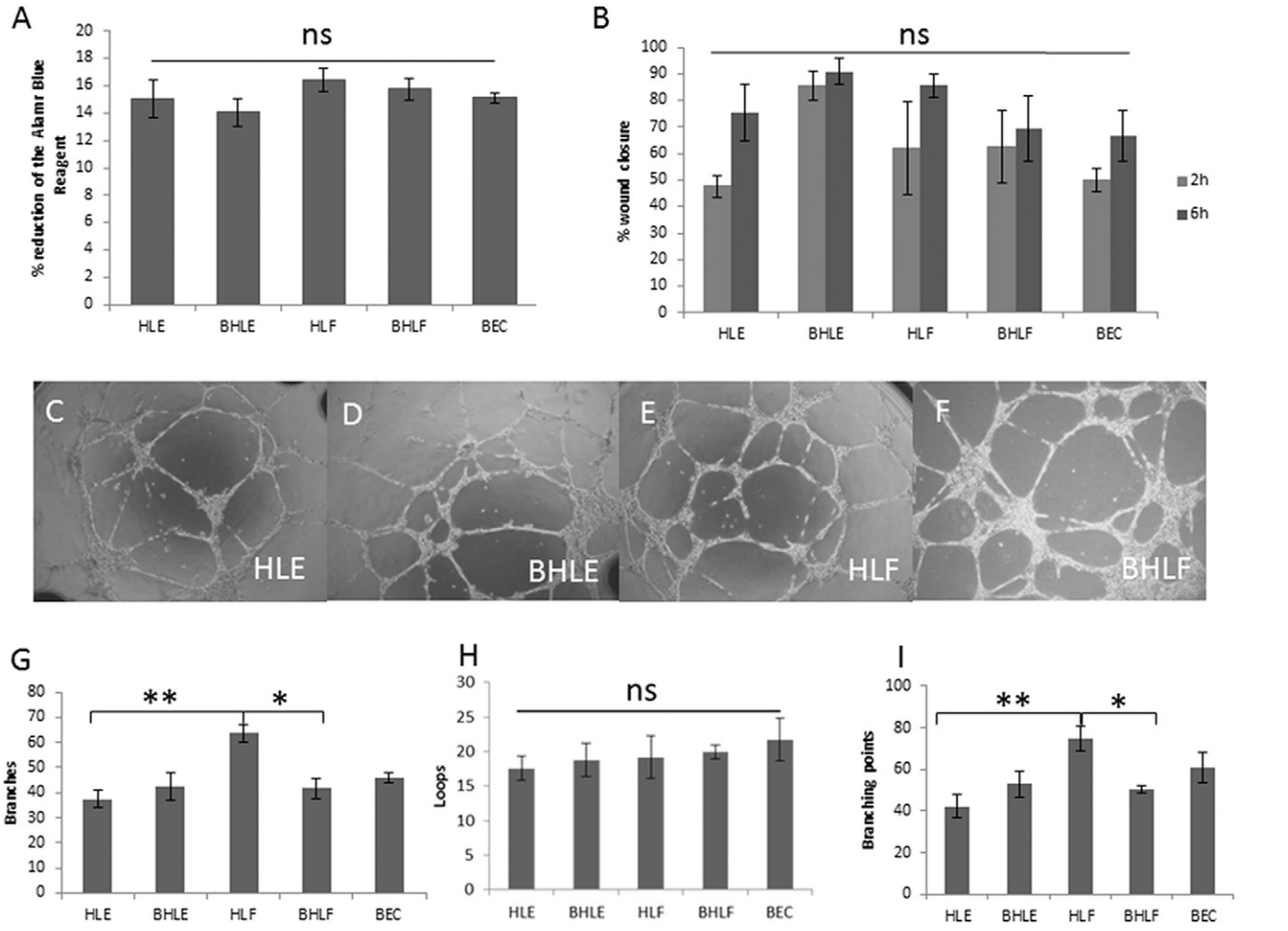

Fig. 4. The paracrine effects of limbal niche cells on blood endothelial cells remain unchanged after UVB. No significant differences were observed in metabolic activity (A) and wound healing (B, 24 h, 48 h) of BEC cells cultured in the CM from all cell groups. Microphotographs from a tube formation assay are displayed in panels C-F.BEC were cultured in CM from HLE, BHLE, HLF and BHLF respecively. CM from HLF induced a significantly higher number of branches (G) and branching points (I) compared to the ones of HLE and BHLF. No change was observed for the number of loops (H).($n = 5$, $^{*}p < 0.05$and $^{**}p < 0,01$).

Similarly, VEGFC levels were down-regulated by 1.8 fold in BHLE compared to HLE ($p < 0.0001$, Fig. 6D). A decrease in BHLF protein levels compared to BHLF only by 1.3-fold was also noted ($p < 0.0001$). A 2.2-fold increase was shown in the protein levels of HLF compared to HLE ($p < 0.0001$).

To investigate the pro-inflammatory signals in each group, a panel of cytokines was selected for ELISA analysis; this included MCP1,TNFαand IFNγ(Fig. 6 E, F, and G respectively).The respective analysis showed that MCP1 levels in HLE CM were significantly lower compared to HLF cells (10-fold, $p < 0.0001$) while they were unchanged for upon HLE irradiation. Also, BHLF cells produced significantly higher amounts of the protein compared to the HLF cells (1.9-fold $p < 0.0001$). IFNγ and TNFαlevels on the other hand, increased significantly in BHLE compared to HLE (5.9-fold, $p < 0.0001$ and 10-fold, $p < 0.0001$ respectively). No detectable TNFα levels were found in all other CM.

4. Discussion:

Corneal homeostasis is maintained as a result of an elegant and dynamic balance where the epithelium and its residing LESC population play a central role. Corneal injury or disease can cause a disruption of LESC function leading to epithelial breakdown and pathologic corneal neovascularization. In the normally avascular cornea, several anti-hem- and anti-lymphangiogenic strategies are expressed (Cursiefen et al., 2006; Bock et al., 2013). A shift in this balance may occur due to various forms of damage including burns, inflammation, infection or neoplasia. The elucidation of the mechanisms involved when this equilibrium is lost may help towards developing more efficient, better targeted treatments for these conditions.

Here we aimed to understand the molecular events involved in disruption of cornea homeostasis as a result of UVB irradiation. Although sun exposure is essential for human health as it aids vitamin D synthesis, extensive exposure, is connected to chronic skin inflammation, skin ageing and melanoma (Reichrath & Reichrath, 2014). UVB-related ocular pathologies include cataract, conjunctival melanoma, macular degeneration (Roberts, 2011; Yam & Kwok, 2014; Sui et al., 2013) and of course pterygium, a benign tumor of the conjunctiva characterized by neovascularization, pain, inflammation and vision loss (Sul et al., 2014). Changes in the histology of the basal epithelium of pterygium samples indicate that damage of the limbal stem cell compartment may be critical for the disease onset. These cells start secretion of extracellular matrix remodeling molecules which aid cell invasion and matrix modification linked with the condition (Chui et al., 2011; Dushku et al., 2001). Here, the direct effects of UVB irradiation on limbal epithelial cells and fibroblasts as well as their subsequent contribution to a pro(lymph)angiogenic and pro-inflammatory milieu usually linked to pterygium were evaluated.

To better understand the effects of the UVB to the limbal niche, we examined both cultured HLE and HLF. HLF are essential components of the niche microenvironment as they support the stem cells by producing suitable extracellular matrix and by providing the paracrine signaling cues that are necessary for them to maintain their phenotype and

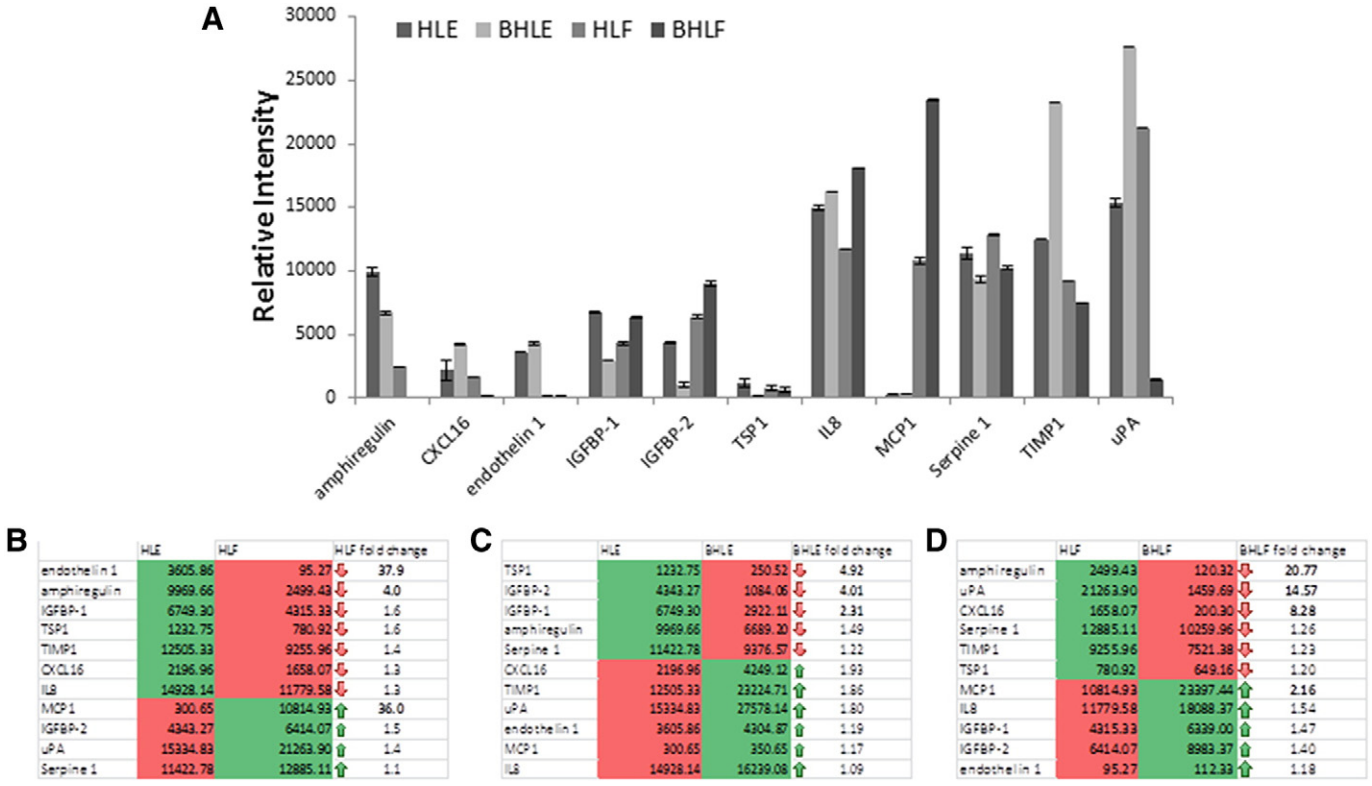

B

	HLE	HLF	HLF fold change
endothelin 1	3605.86	95.27 ⇩	37.9
amphiregulin	9969.66	2499.43 ⇩	4.0
IGFBP-1	6749.30	4315.33 ⇩	1.6
TSP1	1232.75	780.92 ⇩	1.6
TIMP1	12505.33	9255.96 ⇩	1.4
CXCL16	2196.96	1658.07 ⇩	1.3
IL8	14928.14	11779.58 ⇩	1.3
MCP1	300.65	10814.93 ⇧	36.0
IGFBP-2	4343.27	6414.07 ⇧	1.5
uPA	15334.83	21263.90 ⇧	1.4
Serpine 1	11422.78	12885.11 ⇧	1.1

C

	HLE	BHLE	BHLE fold change
TSP1	1232.75	250.52 ⇩	4.92
IGFBP-2	4343.27	1084.06 ⇩	4.01
IGFBP-1	6749.30	2922.11 ⇩	2.31
amphiregulin	9969.66	6689.20 ⇩	1.49
Serpine 1	11422.78	9376.57 ⇩	1.22
CXCL16	2196.96	4249.12 ⇧	1.93
TIMP1	12505.33	23224.71 ⇧	1.86
uPA	15334.83	27578.14 ⇧	1.80
endothelin 1	3605.86	4304.87 ⇧	1.19
MCP1	300.65	350.65 ⇧	1.17
IL8	14928.14	16239.08 ⇧	1.09

D

	HLF	BHLF	BHLF fold change
amphiregulin	2499.43	120.32 ⇩	20.77
uPA	21263.90	1459.69 ⇩	14.57
CXCL16	1658.07	200.30 ⇩	8.28
Serpine 1	12885.11	10259.96 ⇩	1.26
TIMP1	9255.96	7521.38 ⇩	1.23
TSP1	780.92	649.16 ⇩	1.20
MCP1	10814.93	23397.44 ⇧	2.16
IL8	11779.58	18088.37 ⇧	1.54
IGFBP-1	4315.33	6339.00 ⇧	1.47
IGFBP-2	6414.07	8983.37 ⇧	1.40
endothelin 1	95.27	112.33 ⇧	1.18

Fig. 5. UVB irradiation affects angiogenesis- and inflammation-related proteins produced by limbal epithelial cells and limbal fibroblasts. Protein array semiquantification analysis by densitometry is displayed in graph A. and in three heatmaps which include the respective relative intsnsity fold change for each protein (B-D) In heatmap B, limbal epithelial cells are compared with limbal fibroblasts, in C limbal epithelial cells are compared with irradiated limbal epithelial cells and in D limbal fibroblasts are compared with irradiated limbal fibroblasts. Relative intensity changes higher than 2-fold are noted in bold letters (n = 2).

remain in quiescent state (Notara et al., 2010b). For the HLF to be able to provide their supporting role, a physical proximity with the LESCs is necessary. The cell-cell contact is facilitating the communication efficiency of the two populations (Dziasko et al., 2014).

From the apoptosis assessment it became obvious that the epithelial cells were more susceptible to UVB irradiation compared to the fibroblasts as irradiated limbal stem cells showed a higher percentage of dead and apoptotic cells compared to limbal fibroblasts. UVB has been

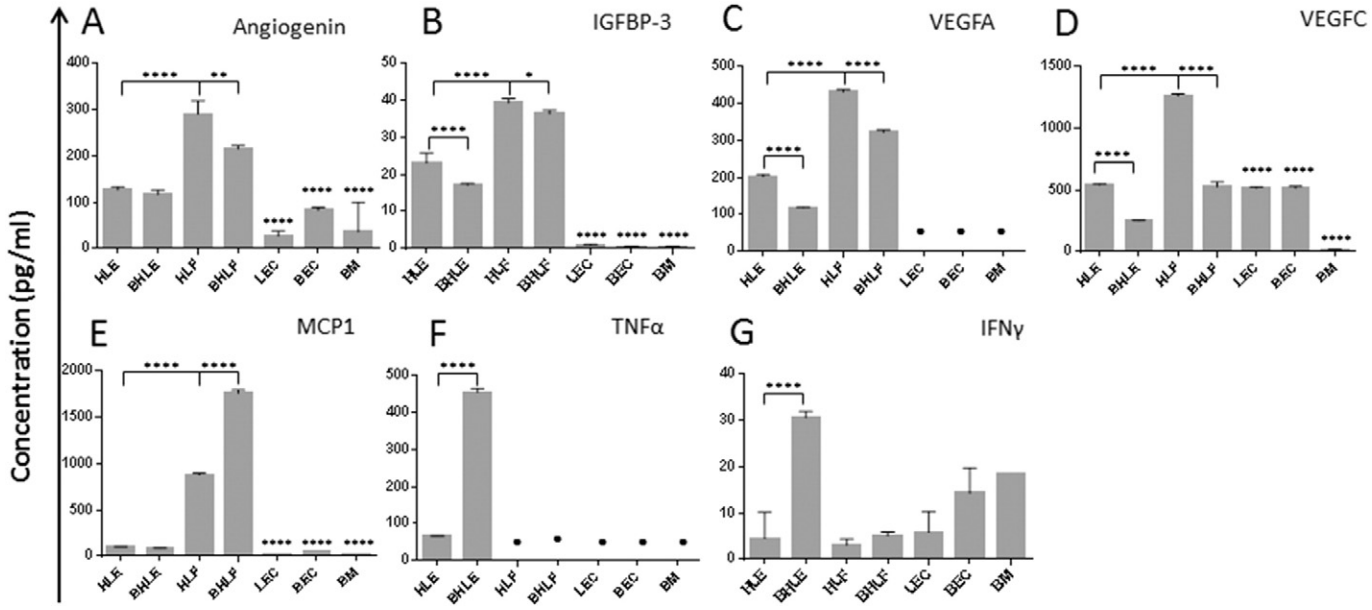

Fig. 6. UVB treatment changes the pro-angiogenic and pro-inflammatory profile of limbal epithelial cells and fibroblasts. Angiogenin (A), IGFBP-3 (B), VEGFA (C), VEGFC (D), MCP1 (E), TNFα (F), and IFNγ (G). Limbal fibroblasts produced significantly higher amounts of Angiogenin, IGFBP-3, VEGFA and VEGFC compared to limbal epithelial cells as well as irradiated limbal fibroblasts. Moreover, there was significantly lower levels of IGFBP-3, VEGFA and VEGFC in irradiated limbal epithelial cells compared to their non-irradiated counterpart. Irradiated limbal epithelial cells produced significantly more TNFα and IFNγ while irradiated limbal fibroblasts exhibited higher levels of MCP1 compared to the non-irradiated ones. (n = 3, *p < 0.05, **p < 0,01 and ***p < 0001 and ****p < 0,0001). Four asterisks (****) situated above bars without brackets correspond to significance in comparison to the HLF group. (● denotes that the protein concentration was under the detectable levels of the assay.)

reported to induce apoptosis to both HLE and HLF (Tong et al., 2006; Xing et al., 2006) although under the current experimental conditions this was observed only in irradiated limbal epithelial cells. Following irradiation and 24 h after plating, both limbal niche cell types exhibited a reduced metabolic activity while still recovering from the UVB insult. However, at 48 h post plating, the alamar blue reduction values for both cell types reached their control level again. Therefore, 48 h post plating was selected as the time-point that conditioned media was collected for analysis and to use in the experiments involving paracrine effect on LEC and BEC cells.

HLE cells which were not UVB irradiated displayed the characteristic phenotype of small cobblestone-like, tightly packed colonies which co-expressed the putative LESC markers including P63a (Di Iorio et al., 2005) and Cytokeratin15 (Meyer-Blazejewska et al., 2010). The expression of β1 integrin by HLE indicates a basal cell phenotype as its presence in corneal epithelial cells has been found to be stronger in the basal layers *in vivo* and in the smaller tightly packed cells *in vitro* (Li et al., 2005). A partial loss of these markers is observed in BHLE cells, coinciding with enlarging cell morphology, an increase in K3-positive cell clusters and a significant drop in %CFE including the %CFE of colonies with a diameter larger than 2 mm. These changes indicate loss of the putative stem cell phenotype following UVB irradiation.

Remarkably, similar changes in marker localization, colony forming efficiency values and morphology are observed in the non-UV treated HLE which are co-cultured with the irradiated limbal fibroblasts (BHLF). The serum-free co-culture model used here, was previously shown to promote expansion of HLE displaying an enhanced putative stem cell like phenotype with an increased colony forming efficiency (Notara et al., 2010b) compared to the routine method of culture on growth arrested 3 T3 fibroblast feeders (Rheinwald & Green, 1975; Detmar et al., 1993). For the first time, it is shown that UVB disrupts the ability of limbal fibroblasts to facilitate expansion of limbal epithelial cells in a co-culture whilst successfully maintaining their putative stem cell phenotype. Increasing evidence suggests that spatial proximity including physical contact between subsets of the limbal fibroblasts and putative stem cells within the niche is essential (Dziasko et al., 2014). The epithelial-fibroblast crosstalk in the limbal niche is fundamental as the latter contribute in mechanisms which prevent stem cell differentiation, such as the BMP/Wnt (Han et al., 2014), TGFβ/BMP (Joyce & Zieske, 1997; Nakatsu et al., 2013)and Notch (Tsai et al., 2014; Kulkarni et al., 2010) pathways. A disruption in the function of HLF, a key cellular component of the limbal microenvironment will be detrimental for the niche function.

After investigating the direct impact of UVB on limbal epithelial cells and limbal fibroblasts, secondary effects on their pro(lymph)angiogenic activity were assessed. Therefore, conditioned media from the cells with and without UVB irradiation was used in functional assays of lymphatic and blood endothelial cells and for protein analysis. The aim was to investigate the synergistic effect of one or more soluble factors produced by the cells on (lymph)angiogenesis. Conditioned medium from HLF induced higher levels of LEC proliferation, wound closure and all parameters of tube network complexity in a tube formation assay. This effect was less pronounced for blood vascular endothelium. These data suggest a previously unreported stronger stimulatory effect of limbal fibroblasts in favor of lymphangiogenesis compared to hemangiogenesis. Earlier studies using a co-culture of an immortalized vascular endothelial cell line with limbal fibroblasts also indicated that the later had a stimulatory effect in tube formation; the opposite was observed in an older study using rabbit epithelial and fibroblast cells to investigate vascular endothelial cell proliferation (Eliason & Elliott, 1987). A proteomic approach in the form of an angiogenesis array as well as individual ELISA analyses were employed to elucidate the mechanisms involved in this response.

The protein analyses data revealed a profile where both pro-angiogenic and anti-angiogenic signals were expressed in different levels by HLE and HLF. Specifically, the pro-angiogenic proteins endothelin 1 and amphiregulin, were strongly down-regulated. Endothelin 1 is both an angiogenesis (Wu et al., 2014; Zhang et al., 2014) and lymphangiogenesis (Spinella et al., 2009; Garrafa et al., 2012) promoter while amphiregulin may enhance lymphangiogenesis in skin (Marino et al., 2013) and hemangiogenesis in normal gut tissue (Shao et al., 2006)as well as in some cancer models (Fontanini et al., 1998; Ma et al., 1999). At the same time, MCP1, angiogenin, IGBP-3, VEGFA and VEGF C were significantly increased in HLF cells. MCP1 is both a pro-angiogenic chemokine (Hong et al., 2005) and a major inducer of monocyte recruitment (Palframan et al., 2001) while angiogenin is a pro-angiogenic growth factor found to stimulate both lymph-angiogenesis and hem-angiogenesis in cancer (Park et al., 2002) and in cornea (Shin et al., 2000; Kim et al., 1999). IGFBP3 is strongly expressed in superficial layers of the corneal epithelium (Robertson et al., 2007) and is upregulated in corneal fibroblasts during myofibroblast differentiation in corneal wound healing (Izumi et al., 2006). VEGFA and VEGFC are also up-regulated in HLF compared to HLE cells. VEGFC is the master regulator in cornea lymphangiogenesis; it is normally expressed in corneal epithelium but the ectopically expressed VEGFR3 acts as a 'sink' preventing VEGFC action and thus maintaining avascularity (Cursiefen et al., 2006; Cursiefen et al., 2005; Bock et al., 2008). VEGFA on the other hand is promoting cornea hem-angiogenesis via VEGFR-2 while also stimulating lymphangiogenesis (Cursiefen et al., 2004a). Given these data, with an emphasis to the VEGFA and VEGFC assessment, it is possible that this protein expression profile is tipping the balance towards a pro-lymphangiogenic and a weaker pro-hem-angiogenic effect of HLF compared to HLE. This also correlated with the outcome of the LEC and BEC functional assays. *In vivo*, since fibroblasts populate the cornea in low numbers compared to epithelial cells, the HLF pro-angiogenic effect observed *in vitro* is not evident. However, in a situation where the fibroblasts in the stroma become hyper-proliferative, like in pterygium (Su et al., 2011; Kim et al., 2013; Almeida Junior et al., 2008), this pro-angiogenic effect from the HLF may contribute to the neovascularization and recurrence of the condition.

After comparing the (lymph)angiogenic effects of HLE and HLF, UVB-induced changes in their protein expression patterns were also assessed. As shown by the protein array assessment, following UVB irradiation of HLF cells amphiregulin, uPA (a strong promoter of angiogenesis (Oh et al., 2003) the expression of which is linked with high risk for cancer metastasis via lymph-angiogenesis (Zhang et al., 2011; Jiang et al., 2012; Zhang et al., 2013)) and CXCL16 (a pro-hem and pro-lymphangiogenic factor (Wente et al., 2008; Buttler et al., 2014)) were strongly down-regulated in BHLF cells. ELISA data showed that angiogenin, IGBP-3, VEGFA and VEGF C also significantly decreased. These results suggest that the pro-angiogenic effect of HLF cells is reversed after UVB irradiation which corresponds to results for LEC proliferation, wound healing and tube formation assay and BEC tube formation assay.

In the case of BHLE on the other hand, a small but significant reduction of IGFBP-3, VEGFA and VEGFC occurred in combination with the decrease of the pro-angiogenic cytokines IGFBP-1 and IGFBP-2 (Giannini et al., 2006; Kluge et al., 1997). TSP1, an inhibitor of corneal lymph and hem-angiogenesis (Cursiefen et al., 2011; Cursiefen et al., 2004b) was also increased. These data, in combination with the LEC and BEC activity assays experiments, suggest that the alterations in the protein profile of HLE cells after UVB treatment were not sufficient to induce a significant effect to these cells.

While investigating the impact of UVB treatment on the angiogenic profile of HLE and HLF cells, changes in the produced inflammatory and macrophage-recruiting cytokines were also evaluated. UVB irradiation increased the pro-inflammatory cytokines TNFα and IFNγ by HLE and MCP1 by HLF. TNFα is a commonly accepted key inflammatory factor (Michalova & Lim, 2008) contributing to vasodilatation, edema, and leukocyte recruitment, which are all commonly associated with the development of cornea neovascularization (Ferrari et al., 2015). IFNγ on the other hand, has been linked with increased angiogenesis via

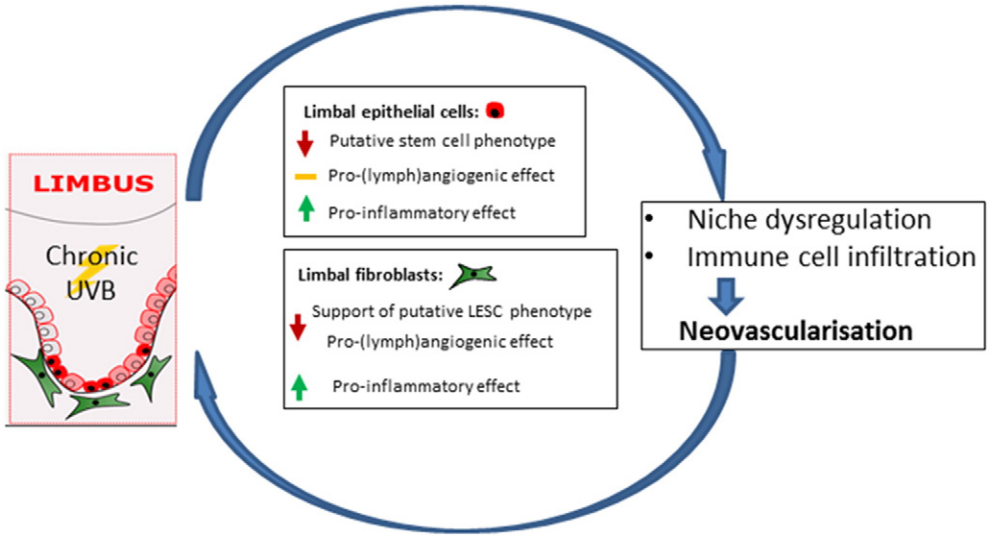

Fig. 7. Schematic representation of the effects of Ultraviolet B irradiation on the limbal niche. UVB irradiation affects limbal epithelial cells by reducing their putative stem cell phenotype as well as increasing their proinflammatory paracrine action. While UVB irradiated limbal fibroblasts reduce their pro-lymphangiogenic effect, they loose their ability to maintain the limbal epithelial stem cell character and they also contribute to inflammation. As a result, the niche function is dissrupted and the increased proinflammatory milieu causes the infiltration of immune cells such as macrophages and neutrophils leading to pathologic hem- and lymphangiogenesis.

induction of VEGF production by macrophages (Lee et al., 2014; Xiong et al., 1998). It is therefore here demonstrated that by producing these cytokines both HLE and HLF cells may contribute to the inflammatory mechanisms taking place in the cornea following UVB irradiation.

Taken together, these observations put forward a double role of the limbal epithelial cells and fibroblasts subsequent to short term UVB insult. A suggested model for this response is summarized in Fig.7. On one hand limbal fibroblasts reduce their pro-angiogenic potential by down-regulating expression of key cytokines such as VEGFA and VEGFC. It is possible that the limbal cell populations put to use a defense mechanism to prevent corneal neovascularization which otherwise could occur after UVB exposure. At the same time, these cells secrete pro-inflammatory and macrophage–recruiting cytokines thus helping in tissue repair but also adding to the inflammatory conditions that propagate (lymph)angiogenesis by promoting infiltration of immune cells populations producing pro-angiogenic growth factors (Hong et al., 2005; Cursiefen et al., 2004a). This pro-inflammatory action, in combination with the decline of the putative stem cell phenotype within the limbal epithelial population may cause an indirect pro(lymph)angiogenic shift in the limbus as a result of UVB exposure (Fig.7). Via recruitment of macrophages, hem- and lymphangiogenesis can be significantly upregulated (Cursiefen et al., 2006; Bock et al., 2013). Long term UVB exposure could therefore contribute to inflammation and pathologic neovascularization both consistent with the progression and recurrence of pterygium. The long term effects of UVB are not assessed here and are the subject of a different investigation. This study highlights the changes that short term UVB treatment induces to the limbal stem cell niche phenotype as well as the functions of its cellular components in the processes indirectly leading to (lymph)angiogenesis via up-regulation of macrophage recruiting cytokines. Macrophages are well known as indirect key regulators of immune-amplification cascades and indirect amplifiers of hem- and lymphangiogenesis via producing VEGFA, C and D (Cursiefen et al., 2005; Cursiefen et al., 2004a). Our results open up new treatment avenues against pterygium recurrence by targeting macrophage recruitment-mediated prolymphangiogenesis.

5. Conclusions:

Short-term UVB irradiation induces limbal stem cell niche disruption both by having a direct effect on the putative stem cell phenotype as well as by impacting on the ability of the accessory niche cells (limbal fibroblasts) to support limbal stem cell maintenance. Moreover, while limbal fibroblasts normally produce soluble mediators that promote blood and lymphatic endothelial cell activity, this effect is reversed following UVB irradiation. At the same time, UVB triggers the production of pro-inflammatory and macrophage recruiting cytokines by both limbal epithelial cells and fibroblasts. These data make evident the quintessential role of limbal epithelial cells and fibroblasts in the response of the niche to UVB as well as subsequent inflammatory and (lymph)angiogenic events. UVB irradiation causes an indirect pro(lymph)angiogenic milieu via up-regulation of macrophage recruiting cytokines.

Acknowledgements

The authors acknowledge Mr. Hans Gunter Simons and Ms. Sabine Hackbarth from the Cornea Bank of the University of Cologne, Cologne for their assistence in this project.

References

Coroneo, M.T., Muller-Stolzenburg, N.W., Ho, A., 1991. Peripheral light focusing by the anterior eye and the ophthalmohelioses. Ophthalmic Surg. 22 (12), 705–711.
Maloof, A.J., Ho, A., Coroneo, M.T., 1994. Influence of corneal shape on limbal light focusing. Invest. Ophthalmol. Vis. Sci. 35 (5), 2592–2598.
Bradley, J.C., Yang, W., Bradley, R.H., Reid, T.W., Schwab, I.R., 2010. The science of pterygia. Br. J. Ophthalmol. 94 (7), 815–820.
Notara, M., Alatza, A., Gilfillan, J., Harris, A.R., Levis, H.J., Schrader, S., et al., 2010. In sickness and in health: corneal epithelial stem cell biology, pathology and therapy. Exp. Eye Res. 90 (2), 188–195.
Notara, M., Daniels, J.T., 2008. Biological principals and clinical potentials of limbal epithelial stem cells. Cell Tissue Res. 331 (1), 135–143.
Ksander, B.R., Kolovou, P.E., Wilson, B.J., Saab, K.R., Guo, Q., Ma, J., et al., 2014. ABCB5 is a limbal stem cell gene required for corneal development and repair. Nature 511 (7509), 353–357.
Barrandon, Y., Green, H., 1987. Three clonal types of keratinocyte with different capacities for multiplication. Proc. Natl. Acad. Sci. U. S. A. 84 (8), 2302–2306.
Chui, J., Coroneo, M.T., Tat, L.T., Crouch, R., Wakefield, D., Di Girolamo, N., 2011. Ophthalmic pterygium: a stem cell disorder with premalignant features. J. Pathol. 178 (2), 817–827.
Di Girolamo, N., Coroneo, M.T., Wakefield, D., 2003. UVB-elicited induction of MMP-1 expression in human ocular surface epithelial cells is mediated through the ERK1/2 MAPK-dependent pathway. Invest. Ophthalmol. Vis. Sci. 44 (11), 4705–4714.
Dushku, N., Reid, T.W., 1994. Immunohistochemical evidence that human pterygia originate from an invasion of vimentin-expressing altered limbal epithelial basal cells. Curr. Eye Res. 13 (7), 473–481.

Dushku, N., John, M.K., Schultz, G.S., Reid, T.W., 2001. Pterygia pathogenesis: corneal invasion by matrix metalloproteinase expressing altered limbal epithelial basal cells. Arch. Ophthalmol. 119 (5), 695–706.

Cimpean, A.M., Sava, M.P., Raica, M., 2013. DNA damage in human pterygium: one-shot multiple targets. Mol. Vis. 19, 348–356.

Notara, M., Shortt, A.J., O'Callaghan, A.R., Daniels, J.T., 2013. The impact of age on the physical and cellular properties of the human limbal stem cell niche. Age (Dordr.) 35 (2), 289–300.

Corsini, E., Sangha, N., Feldman, S.R., 1997. Epidermal stratification reduces the effects of UVB (but not UVA) on keratinocyte cytokine production and cytotoxicity. Photodermatol. Photoimmunol. Photomed. 13 (4), 147–152.

Di Girolamo, N., Kumar, R.K., Coroneo, M.T., Wakefield, D., 2002. UVB-mediated induction of interleukin-6 and −8 in pterygia and cultured human pterygium epithelial cells. Invest. Ophthalmol. Vis. Sci. 43 (11), 3430–3437.

Kennedy, M., Kim, K.H., Harten, B., Brown, J., Planck, S., Meshul, C., et al., 1997. Ultraviolet irradiation induces the production of multiple cytokines by human corneal cells. Invest. Ophthalmol. Vis. Sci. 38 (12), 2483–2491.

Fukuhara, J., Kase, S., Ohashi, T., Ando, R., Dong, Z., Noda, K., et al., 2013. Expression of vascular endothelial growth factor C in human pterygium. Histochem. Cell Biol. 139 (2), 381–389.

Lee, D.H., Cho, H.J., Kim, J.T., Choi, J.S., Joo, C.K., 2001. Expression of vascular endothelial growth factor and inducible nitric oxide synthase in pterygia. Cornea 20 (7), 738–742.

Kria, L., Ohira, A., Amemiya, T., 1996. Immunohistochemical localization of basic fibroblast growth factor, platelet derived growth factor, transforming growth factor-beta and tumor necrosis factor-alpha in the pterygium. Acta Histochem. 98 (2), 195–201.

Di Girolamo, N., Coroneo, M., Wakefield, D., 2005. Epidermal growth factor receptor signaling is partially responsible for the increased matrix metalloproteinase-1 expression in ocular epithelial cells after UVB radiation. J. Pathol. 167 (2), 489–503.

Li, D.Q., Lee, S.B., Gunja-Smith, Z., Liu, Y., Solomon, A., Meller, D., et al., 2001. Overexpression of collagenase (MMP-1) and stromelysin (MMP-3) by pterygium head fibroblasts. Arch. Ophthalmol. 119 (1), 71–80.

Cursiefen, C., Chen, L., Saint-Geniez, M., Hamrah, P., Jin, Y., Rashid, S., et al., 2006. Nonvascular VEGF receptor 3 expression by corneal epithelium maintains avascularity and vision. Proc. Natl. Acad. Sci. U. S. A. 103 (30), 11405–11410.

Ling, S., Li, Q., Lin, H., Li, W., Wang, T., Ye, H., et al., 2012. Comparative evaluation of lymphatic vessels in primary versus recurrent pterygium. Eye (Lond.). 26 (11), 1451–1458.

Ling, S., Liang, L., Lin, H., Li, W., Xu, J., 2012. Increasing lymphatic microvessel density in primary pterygia. Arch. Ophthalmol. 130 (6), 735–742.

Notara, M., Shortt, A.J., Galatowicz, G., Calder, V., Daniels, J.T., 2010. IL6 and the human limbal stem cell niche: a mediator of epithelial-stromal interaction. Stem Cell Res. 5 (3), 188–200.

Bock, F., Maruyama, K., Regenfuss, B., Hos, D., Steven, P., Heindl, L.M., et al., 2013. Novel anti(lymph)angiogenic treatment strategies for corneal and ocular surface diseases. Prog. Retin. Eye Res. 34, 89–124.

Reichrath, J., Reichrath, S., 2014. Sunlight, vitamin D and malignant melanoma: an update. Adv. Exp. Med. Biol. 810, 390–405.

Roberts, J.E., 2011. Ultraviolet radiation as a risk factor for cataract and macular degeneration. Eye Contact Lens 37 (4), 246–249.

Yam, J.C., Kwok, A.K., 2014. Ultraviolet light and ocular diseases. Int. Ophthalmol. 34 (2), 383–400.

Sui, G.Y., Liu, G.C., Liu, G.Y., Gao, Y.Y., Deng, Y., Wang, W.Y., et al., 2013. Is sunlight exposure a risk factor for age-related macular degeneration? A systematic review and meta-analysis. Br. J. Ophthalmol. 97 (4), 389–394.

Sul, S., Korkmaz, S., Novruzlu, S., 2014. Seasonal effects on pterygium surgery outcome: implications for the role of sunlight exposure. Cornea 33 (5), 504–506.

Dziasko, M.A., Armer, H.E., Levis, H.J., Shortt, A.J., Tuft, S., Daniels, J.T., 2014. Localisation of epithelial cells capable of holoclone formation in vitro and direct interaction with stromal cells in the native human limbal crypt. PLoS One 9 (4), e94283.

Tong, L., Chen, Z., De Paiva, C.S., Beuerman, R., Li, D.Q., Pflugfelder, S.C., 2006. Transglutaminase participates in UVB-induced cell death pathways in human corneal epithelial cells. Invest. Ophthalmol. Vis. Sci. 47 (10), 4295–4301.

Xing, D., Sun, X., Li, J., Cui, M., Tan-Allen, K., Bonanno, J.A., 2006. Hypoxia preconditioning protects corneal stromal cells against induced apoptosis. Exp. Eye Res. 82 (5), 780–787.

Di Iorio, E., Barbaro, V., Ruzza, A., Ponzin, D., Pellegrini, G., De Luca, M., 2005. Isoforms of DeltaNp63 and the migration of ocular limbal cells in human corneal regeneration. Proc. Natl. Acad. Sci. U. S. A. 102 (27), 9523–9528.

Meyer-Blazejewska, E.A., Kruse, F.E., Bitterer, K., Meyer, C., Hofmann-Rummelt, C., Wunsch, P.H., et al., 2010. Preservation of the limbal stem cell phenotype by appropriate culture techniques. Invest. Ophthalmol. Vis. Sci. 51 (2), 765–774.

Li, D.Q., Chen, Z., Song, X.J., de Paiva, C.S., Kim, H.S., Pflugfelder, S.C., 2005. Partial enrichment of a population of human limbal epithelial cells with putative stem cell properties based on collagen type IV adhesiveness. Exp. Eye Res. 80 (4), 581–590.

Rheinwald, J.G., Green, H., 1975. Serial cultivation of strains of human epidermal keratinocytes: the formation of keratinizing colonies from single cells. Cell 6 (3), 331–343.

Detmar, M., Schaart, F.M., Blume, U., Orfanos, C.E., 1993. Culture of hair matrix and follicular keratinocytes. J. Invest. Dermatol. 101 (1 Suppl), 130s–134s.

Han, B., Chen, S.Y., Zhu, Y.T., Tseng, S.C., 2014. Integration of BMP/Wnt signaling to control clonal growth of limbal epithelial progenitor cells by niche cells. Stem Cell Res. 12 (2), 562–573.

Joyce, N.C., Zieske, J.D., 1997. Transforming growth factor-beta receptor expression in human cornea. Invest. Ophthalmol. Vis. Sci. 38 (10), 1922–1928.

Nakatsu, M.N., Vartanyan, L., Vu, D.M., Ng, M.Y., Li, X., Deng, S.X., 2013. Preferential biological processes in the human limbus by differential gene profiling. PLoS One 8 (4), e61833.

Tsai, T.H., Sun, M.H., Ho, T.C., Ma, H.I., Liu, M.Y., Tsao, Y.P., 2014. Notch prevents transforming growth factor-beta-assisted epithelial-mesenchymal transition in cultured limbal progenitor cells through the induction of Smad7. Mol. Vis. 20, 522–534.

Kulkarni, B.B., Tighe, P.J., Mohammed, I., Yeung, A.M., Powe, D.G., Hopkinson, A., et al., 2010. Comparative transcriptional profiling of the limbal epithelial crypt demonstrates its putative stem cell niche characteristics. BMC Genomics 11, 526.

Eliason, J.A., Elliott, J.P., 1987. Proliferation of vascular endothelial cells stimulated in vitro by corneal epithelium. Invest. Ophthalmol. Vis. Sci. 28 (12), 1963–1969.

Wu, M.H., Huang, C.Y., Lin, J.A., Wang, S.W., Peng, C.Y., Cheng, H.C., et al., 2014. Endothelin-1 promotes vascular endothelial growth factor-dependent angiogenesis in human chondrosarcoma cells. Oncogene 33 (13), 1725–1735.

Zhang, J., Yang, W., Hu, B., Wu, W., Fallon, M.B., 2014. Endothelin-1 activation of the endothelin B receptor modulates pulmonary endothelial CX3CL1 and contributes to pulmonary angiogenesis in experimental hepatopulmonary syndrome. J. Pathol. 184 (6), 1706–1714.

Spinella, F., Garrafa, E., Di Castro, V., Rosano, L., Nicotra, M.R., Caruso, A., et al., 2009. Endothelin-1 stimulates lymphatic endothelial cells and lymphatic vessels to grow and invade. Cancer Res. 69 (6), 2669–2676.

Garrafa, E., Caprara, V., Di Castro, V., Rosano, L., Bagnato, A., Spinella, F., 2012. Endothelin-1 cooperates with hypoxia to induce vascular-like structures through vascular endothelial growth factor-C, −D and -a in lymphatic endothelial cells. Life Sci. 91 (13–14), 638–643.

Marino, D., Angehrn, Y., Klein, S., Riccardi, S., Baenziger-Tobler, N., Otto, V.I., et al., 2013. Activation of the epidermal growth factor receptor promotes lymphangiogenesis in the skin. J. Dermatol. Sci. 71 (3), 184–194.

Shao, J., Sheng, G.G., Mifflin, R.C., Powell, D.W., Sheng, H., 2006. Roles of myofibroblasts in prostaglandin E2-stimulated intestinal epithelial proliferation and angiogenesis. Cancer Res. 66 (2), 846–855.

Fontanini, G., De Laurentiis, M., Vignati, S., Chine, S., Lucchi, M., Silvestri, V., et al., 1998. Evaluation of epidermal growth factor-related growth factors and receptors and of neoangiogenesis in completely resected stage I-IIIA non-small-cell lung cancer: amphiregulin and microvessel count are independent prognostic indicators of survival. Clin. Cancer Res. 4 (1), 241–249.

Ma, L., Gauville, C., Berthois, Y., Millot, G., Johnson, G.R., Calvo, F., 1999. Antisense expression for amphiregulin suppresses tumorigenicity of a transformed human breast epithelial cell line. Oncogene 18 (47), 6513–6520.

Hong, K.H., Ryu, J., Han, K.H., 2005. Monocyte chemoattractant protein-1-induced angiogenesis is mediated by vascular endothelial growth factor-a. Blood 105 (4), 1405–1407.

Palframan, R.T., Jung, S., Cheng, G., Weninger, W., Luo, Y., Dorf, M., et al., 2001. Inflammatory chemokine transport and presentation in HEV: a remote control mechanism for monocyte recruitment to lymph nodes in inflamed tissues. J. Exp. Med. 194 (9), 1361–1373.

Park, Y.W., Kim, S.M., Min, B.G., Park, I.W., Lee, S.K., 2002. Lymphangioma involving the mandible: immunohistochemical expressions for the lymphatic proliferation. J. Oral Pathol. Med. 31 (5), 280–283.

Shin, S.H., Kim, J.C., Chang, S.I., Lee, H., Chung, S.I., 2000. Recombinant kringle 1–3 of plasminogen inhibits rabbit corneal angiogenesis induced by angiogenin. Cornea 19 (2), 212–217.

Kim, J.H., Kim, J.C., Shin, S.H., Chang, S.I., Lee, H.S., Chung, S.I., 1999. The inhibitory effects of recombinant plasminogen kringle 1–3 on the neovascularization of rabbit cornea induced by angiogenin, bFGF, and VEGF. Exp. Mol. Med. 31 (4), 203–209.

Robertson, D.M., Ho, S.I., Hansen, B.S., Petroll, W.M., Cavanagh, H.D., 2007. Insulin-like growth factor binding protein-3 expression in the human corneal epithelium. Exp. Eye Res. 85 (4), 492–501.

Izumi, K., Kurosaka, D., Iwata, T., Oguchi, Y., Tanaka, Y., Mashima, Y., et al., 2006. Involvement of insulin-like growth factor-I and insulin-like growth factor binding protein-3 in corneal fibroblasts during corneal wound healing. Invest. Ophthalmol. Vis. Sci. 47 (2), 591–598.

Cursiefen, C., Ikeda, S., Nishina, P.M., Smith, R.S., Ikeda, A., Jackson, D., et al., 2005. Spontaneous corneal hem- and lymphangiogenesis in mice with destrin-mutation depend on VEGFR3 signaling. J. Pathol. 166 (5), 1367–1377.

Bock, F., Onderka, J., Dietrich, T., Bachmann, B., Pytowski, B., Cursiefen, C., 2008. Blockade of VEGFR3-signalling specifically inhibits lymphangiogenesis in inflammatory corneal neovascularisation. Graefe's archive for clinical and experimental ophthalmology = Albrecht von Graefes Archiv fur klinische und experimentelle. Ophthalmologie 246 (1), 115–119.

Cursiefen, C., Chen, L., Borges, L.P., Jackson, D., Cao, J., Radziejewski, C., et al., 2004. VEGF-a stimulates lymphangiogenesis and hemangiogenesis in inflammatory neovascularization via macrophage recruitment. J. Clin. Invest. 113 (7), 1040–1050.

Su, Y., Wang, F., Qi, H., Zhao, S.G., Li, X., Cui, H., 2011. Small interfering RNA targeting of S phase kinase-interacting protein 2 inhibits cell proliferation of pterygium fibroblasts. Mol. Vis. 17, 247–256.

Kim, K.W., Park, S.H., Wee, S.W., Kim, J.C., 2013. Overexpression of angiogenin in pterygium body fibroblasts and its association with proliferative potency. Invest. Ophthalmol. Vis. Sci. 54 (9), 6355–6362.

Almeida Junior, G.C., Frederico, F.B., Watanabe, K.P., Garcia, T.V., Iquejiri, A.Y., Cury, P.M., et al., 2008. Evaluation of epithelial cell proliferating activity and fibroblast nuclear kariometry in recurrent pterygium treated with mitomycin C. Arq. Bras. Oftalmol. 71 (4), 568–575.

Oh, C.W., Hoover-Plow, J., Plow, E.F., 2003. The role of plasminogen in angiogenesis in vivo. J. Thromb. Haemost. 1 (8), 1683–1687.

Zhang, Z., Pan, J., Li, L., Wang, Z., Xiao, W., Li, N., 2011. Survey of risk factors contributed to lymphatic metastasis in patients with oral tongue cancer by immunohistochemistry. J. Oral Pathol. Med. 40 (2), 127–134.

Jiang, J.T., Zhang, L.F., Zhou, B., Zhang, S.Q., Li, S.M., Zhang, W., et al., 2012. Relationships of uPA and VEGF expression in esophageal cancer and microvascular density with tumorous invasion and metastasis. Asian Pac. J. Cancer Prev. 13 (7), 3379–3383.

Zhang, W., Ling, D., Tan, J., Zhang, J., Li, L., 2013. Expression of urokinase plasminogen activator and plasminogen activator inhibitor type-1 in ovarian cancer and its clinical significance. Oncol. Rep. 29 (2), 637–645.

Wente, M.N., Gaida, M.M., Mayer, C., Michalski, C.W., Haag, N., Giese, T., et al., 2008. Expression and potential function of the CXC chemokine CXCL16 in pancreatic ductal adenocarcinoma. Int. J. Oncol. 33 (2), 297–308.

Buttler, K., Badar, M., Seiffart, V., Laggies, S., Gross, G., Wilting, J., et al., 2014. De novo hemand lymphangiogenesis by endothelial progenitor and mesenchymal stem cells in immunocompetent mice. Cell. Mol. Life Sci. 71 (8), 1513–1527.

Giannini, S., Cresci, B., Manuelli, C., Pala, L., Rotella, C.M., 2006. Diabetic microangiopathy: IGFBP control endothelial cell growth by a common mechanism in spite of their species specificity and tissue peculiarity. J. Endocrinol. Investig. 29 (8), 754–763.

Kluge, A., Zimmermann, R., Weihrauch, D., Mohri, M., Sack, S., Schaper, J., et al., 1997. Coordinate expression of the insulin-like growth factor system after microembolisation in porcine heart. Cardiovasc. Res. 33 (2), 324–331.

Cursiefen, C., Maruyama, K., Bock, F., Saban, D., Sadrai, Z., Lawler, J., et al., 2011. Thrombospondin 1 inhibits inflammatory lymphangiogenesis by CD36 ligation on monocytes. J. Exp. Med. 208 (5), 1083–1092.

Cursiefen, C., Masli, S., Ng, T.F., Dana, M.R., Bornstein, P., Lawler, J., et al., 2004. Roles of thrombospondin-1 and −2 in regulating corneal and iris angiogenesis. Invest. Ophthalmol. Vis. Sci. 45 (4), 1117–1124.

Michalova, K., Lim, L., 2008. Biologic agents in the management of inflammatory eye diseases. Curr. Allergy Asthma Rep. 8 (4), 339–347.

Ferrari, G., Bignami, F., Rama, P., 2015. Tumor necrosis factor-alpha inhibitors as a treatment of corneal hemangiogenesis and lymphangiogenesis. Eye Contact Lens 41 (2), 72–76.

Lee, H., Schlereth, S.L., Park, E.Y., Emami-Naeini, P., Chauhan, S.K., Dana, R., 2014. A novel pro-angiogenic function for interferon-gamma-secreting natural killer cells. Invest. Ophthalmol. Vis. Sci. 55 (5), 2885–2892.

Xiong, M., Elson, G., Legarda, D., Leibovich, S.J., 1998. Production of vascular endothelial growth factor by murine macrophages: regulation by hypoxia, lactate, and the inducible nitric oxide synthase pathway. J. Pathol. 153 (2), 587–598.